

A first-order quasi-SV-wave propagator in 2-dimensional vertical transversely isotropic (VTI) media

He Liu and Kristopher Innanen

ABSTRACT

The propagation of elastic waves in formations has been widely investigated in the development of seismic exploration. In a typical transversely isotropic medium (e.g., vertical transversely isotropic-VTI medium), qP- and qSV-waves are intrinsically coupled as described in elastic wave equations. Therefore, coupled qP-wave energy will inevitably contaminate the imaging results from performing elastic reverse time migration (ERTM) and imaging algorithms to qSV-mode waves. Other than directly separate qS-mode waves from full elastic waves in anisotropic media, some researchers have tried to find an alternative way to solve it by the forward simulation of pure-qSV-mode waves. In this study, we propose a first-order wave propagator of pseudo-pure-qSV-mode wave in 2D heterogeneous VTI media, which can be easily employed for the simulation of qSV-mode wave propagation with staggered-grid finite difference scheme. This propagator will directly suppress qP-mode wave energy through projecting the wavefields onto isotropic references of local polarization direction. By further correction of projection deviation of simulated wavefield components, residual qP-waves will be completely eliminated and separated scalar pseudo-pure-qSV-mode waves can be achieved. We have performed the algorithm to isotropic medium, VTI media with weak/strong anisotropy, a two-layer VTI model and part of heterogeneous SEG/Hess VTI model, the synthetic results demonstrate the validity and feasibility of this algorithm. In addition, the more efficient and more stable first-order Hybrid-PML can be directly implemented in this staggered-grid finite difference algorithm, which shows better performance in the wavefield propagation simulation in VTI media with strong anisotropy.

INTRODUCTION

Elastic reverse time migration (ERTM) for seismic multicomponent data has been used to image underground geological structures. However, applying ERTM and imaging algorithms to qP- and qS-mode wavefields will inevitably introduce crosstalk and hence contaminate the imaging results. Yan and Sava (2008b) suggest using imaging conditions based on elastic potentials, which requires cross correlation of separated mode waves. Many authors have been working on the research about how to separate P- and S-wavefields. The basic idea of wavefield separation method is to project the displacement vector wavefield U onto the polarization vectors of P- and S-mode waves. Helmholtz decomposition (Morse and Feshbach, 1954) calculates potentials to determine decomposed vector modes, but this is applicable only for isotropic media and is not able to completely separate mode waves in anisotropic media. In general 2D anisotropic media, P- and SV-mode waves are intrinsically coupled and their polarization direction are no longer parallel or perpendicular to the propagation direction, so they are called ‘quasi-P’ and ‘quasi-SV’ waves, respectively. Rommel (1994) propose to calculate the polarization vectors of qP- and qSV-mode waves by solving the Christoffel equation with local elastic parameters or Thomsen parameters. Polarization vectors of qP-wave can also be calculated by the rotation of

wave vector with a deviation angle, where Thomson parameters can also apply (Tsvankin, 2012). Yoon and Marfurt (2006) propose an efficient way to estimate local wave vectors directions with Poynting vectors method. Based on Helmholtz theory (Aki and Richards, 2002), Dellinger and Etgen (1990) and Dellinger (1991) propose to separate scalar P- and S-mode waves from displacement vector wavefield U by applying a divergence and a curl operation in wavenumber domain, respectively. However, this algorithm only works in homogeneous media, since in heterogeneous media, the polarization components are no longer constant in the x - and z - directions (Yan and Sava, 2008a, 2009). Yan and Sava (2008a, 2009) propose a nonstationary separation method for 2D VTI media, which transforms the wavenumber domain operators into space domain and obtain the space domain pseudo-derivative operators, this algorithm will overcome the shortcoming of wavenumber domain method and can separate qP- and qS-mode waves completely even in media with velocity varying spatially. Zhou and Wang (2016a,b) propose an efficient wave mode separation operators in anisotropic media, which are constructed by local rotation of wave vector polarization. The deviation angle between normal and qP-wave's polarization direction is spatially estimated using Poynting vectors (Dickens and Winbow, 2011).

Beside of the wavefield separation methods, there is an alternative approach to simulate separated P- and S-wave propagation. Since in isotropic media, P- and S-mode waves polarize parallelly and perpendicularly to the propagation direction respectively, Jianlei et al. (2007) propose to simulate P- and S-mode waves with fully decoupled first-order P- and S-wave equations with staggered-grid finite-difference scheme. However, in general anisotropic media, P- and S-mode waves are intrinsically coupled, this algorithm is only practical in isotropic media. In anisotropic media, Cheng and Kang (2016) propose an alternative approach for the simulation of separated qSV-mode waves for forward modeling, migration and waveform inversion, which splits wavefield separation procedure into a two-steps scheme. First, perform a similarity transform to Christoffel matrix of VTI medium to project the wavefield onto isotropic references to derive the second-order pseudo-pure-mode qSV-mode wave equations, which accurately describes the kinematics of qSV-mode wave and seriously suppress qP-waves when the pseudo-pure-mode wavefield components are summed. Second, perform a normalized filtering algorithm to further project synthetic wavefields onto the polarization direction of qSV-waves. Through this two-steps procedure, the residual energy of the qP-mode waves will be completely removed and pseudo-pure-mode qSV-mode waves will be acquired. In this study, to adopt staggered-grid finite difference scheme, we propose to further reduce the order of second-order equations and achieve the first-order equations of qSV-mode wave. Fortunately, as Zhang and McMechan (2010) pointed out, velocity fields can be separated as well as displacement fields. Following the principles of Virieux (1984, 1986), we introduce and distribute the velocity fields and stress fields on a 2D staggered grid, in this way staggered-grid scheme can be employed in the first-order equations and corresponding finite difference iterative format can be achieved. In addition, first-order Hybrid-PML proposed by Zhang et al. (2014) can also be employed straight forward in this algorithm, which will help to better suppress artificial reflections in the wavefield simulation in strongly anisotropic media.

This paper is organized as follows: first, we perform a similarity transform to the Christoffel matrix of a 2D VTI medium to project the wavefield onto isotropic references and derive the second-order pseudo-pure-mode qSV-mode wave equations; second, we in-

produce velocity and stress fields as intermediate variables and further reduce the order of the equations, thus we obtain the first-order pseudo-pure-mode qSV-mode wave equations; third, we perform a space filtering algorithm to synthetic qSV-mode wavefields, which will completely remove residual qP-mode energy. Finally, we perform this new algorithm to isotropic medium, VTI media with weak/strong anisotropy and a two-layer VTI model, heterogeneous Hess VTI model and present the synthetic wavefields. Through the synthetic examples, we demonstrate that this algorithm is valid for simulating pseudo-pure-mode qSV-wave propagation with further polarization-based projection. Through the snapshots of wavefield propagating at different time, we demonstrate that first-order Hybrid-PML is applicable in our algorithm with excellent performance.

First-Order Propagator of Pseudo-Pure-qSV-Mode Waves in 2D VTI Media

Based on Helmholtz theory (Aki and Richards, 2002), a vector wavefield $U = \{U_x, U_z\}$ in isotropic media can be decomposed into P-wavefield (curl-free) and S-wavefield (divergence-free)

$$U = U^P + U^S, \quad (1)$$

where U^S satisfies $\nabla \cdot U^S = 0$. Hence in isotropic media, scalar S-mode wave can be separated from displacement vector wavefield U by applying a curl operation (Dellinger and Etgen, 1990; Dellinger, 1991): $U^S = \nabla \times U$. In the wavenumber domain, it can be equivalently expressed as a cross product that essentially projects the wavefield \tilde{U} onto the wave vector K :

$$\tilde{U}^S = i K \times \tilde{U}. \quad (2)$$

In 2D isotropic media, the wavenumber $K = (k_x, k_z)^T$ is not only the wave propagation direction, but also the P-mode wave polarization direction. However, in anisotropic media, the polarization directions of qP- and qSV-mode waves are no longer parallel or perpendicular to the propagation direction. So in anisotropic media, equation 2 can be rewritten as

$$\tilde{U}^{SV} = i a^{qP} \times \tilde{U}, \quad (3)$$

where $a^{qP} = (a_x^{qP}, a_z^{qP})^T$ is the polarization vector of qP-mode waves. To provide more flexibility for wave propagation characterization in anisotropic media, Cheng and Kang (2013, 2016) propose to split this projection separation procedure into a two-steps scheme. First, project the original qSV-wavefield onto isotropic references through the introduction of a similarity transformation to Christoffel matrix G

$$\tilde{G}_{qSV} = M_{SV} G M_{SV}^{-1}, \quad (4)$$

where

$$M_{SV} = \begin{bmatrix} k_x & k_z & 0 \\ 0 & -k_x^2 & \end{bmatrix}. \quad (5)$$

According to the elastic matrix of 2D VTI medium,

$$C = \begin{bmatrix} C_{11} & C_{13} & \\ C_{13} & C_{33} & \\ & & C_{44} \end{bmatrix}. \quad (6)$$

Christoffel matrix \tilde{G} has the form as below:

$$\tilde{G} = \begin{bmatrix} C_{11} k_x^2 + C_{44} k_z^2 & (C_{13} + C_{44}) k_x k_z \\ (C_{13} + C_{44}) k_x k_z & C_{44} k_x^2 + C_{33} k_z^2 \end{bmatrix}. \quad (7)$$

After the similarity transform of Christoffel matrix,

$$\tilde{G}_{qSV} = \begin{bmatrix} C_{11} k_x^2 + C_{44} k_z^2 & -(C_{13} + C_{44}) k_x k_z \\ -(C_{13} + C_{44}) k_x k_z & C_{44} k_x^2 + C_{33} k_z^2 \end{bmatrix}. \quad (8)$$

In this way, equivalent Christoffel equation of qSV-mode waves is derived as below:

$$\tilde{G}^{qSV} \tilde{U}^{qSV} = \rho \omega^2 \tilde{U}^{qSV}. \quad (9)$$

Hence, through inverse Fourier transform of equation 9, second-order pseudo-pure-qSV-mode wave equations of the transformed wavefields \bar{U}^{qSV} can be obtained:

$$\rho \frac{\partial^2 \bar{U}^{qSV}}{\partial t^2} = \bar{G} \bar{U}^{qSV}. \quad (10)$$

According to the elastic matrix of 2D VTI media, the second-order qSV-mode wave equation 10 can be expressed as below:

$$\begin{aligned} \rho \frac{\partial^2 u_x}{\partial t^2} &= C_{11} \frac{\partial^2 u_x}{\partial x^2} + C_{44} \frac{\partial^2 u_x}{\partial z^2} - (C_{13} + C_{44}) \frac{\partial^2 u_z}{\partial z^2} \\ \rho \frac{\partial^2 u_z}{\partial t^2} &= C_{33} \frac{\partial^2 u_z}{\partial z^2} + C_{44} \frac{\partial^2 u_z}{\partial x^2} - (C_{13} + C_{44}) \frac{\partial^2 u_x}{\partial x^2}. \end{aligned} \quad (11)$$

It can be seen that there are no mixed derivatives terms in the equations above, and thus different from those in first-order elastic wave equations. Compared to second-order equations with finite difference method, first-order equations with staggered-grid scheme can better suppress the numerical dispersion with a finer grid, while achieving higher accuracy and efficiency. In this study, we propose to further reduce the order of the equations and turn them into first-order equations by following procedures. First, we introduce velocity fields v_x and v_z as intermediate variables and let

$$\begin{aligned} \frac{\partial u_x}{\partial t} &= v_x \\ \frac{\partial u_z}{\partial t} &= v_z \end{aligned} \quad (12)$$

and hence keeps the same relationship between displacement fields and velocity fields as they are in original elastic wave equations. For qSV-mode wave equation 11, we further

introduce variables (Liu et al., 2018): σ_{xx} , σ_{zz} , σ_{xz} , σ_{zx} and let

$$\begin{aligned}\rho \frac{\partial \sigma_{xx}}{\partial t} &= C_{11} \frac{\partial v_x}{\partial x} \\ \rho \frac{\partial \sigma_{zz}}{\partial t} &= C_{33} \frac{\partial v_z}{\partial z} \\ \rho \frac{\partial \sigma_{xz}}{\partial t} &= C_{44} \frac{\partial v_x}{\partial z} - (C_{13} + C_{44}) \frac{\partial v_z}{\partial z} \\ \rho \frac{\partial \sigma_{zx}}{\partial t} &= C_{44} \frac{\partial v_z}{\partial x} - (C_{13} + C_{44}) \frac{\partial v_x}{\partial x}\end{aligned}\tag{13}$$

What's worthy to notice is that, σ_{xz} and σ_{zx} have to be introduced separately, but they can be distributed at the same grid points. Then we substitute equation 13 into equation 11, we get:

$$\begin{aligned}\rho \frac{\partial v_x}{\partial t} &= \frac{\partial \sigma_{xx}}{\partial x} + \frac{\partial \sigma_{xz}}{\partial z} \\ \rho \frac{\partial v_z}{\partial t} &= \frac{\partial \sigma_{zx}}{\partial x} + \frac{\partial \sigma_{zz}}{\partial z}\end{aligned}\tag{14}$$

In this way, we derive the first-order pseudo-pure-mode qSV-mode wave equations. In addition, applying the Thomsen notation (Thomsen, 1986):

$$\begin{aligned}C_{11} &= (1 + 2\epsilon)\rho v_{p0}^2 \\ C_{33} &= \rho v_{p0}^2 \\ C_{44} &= \rho v_{s0}^2 \\ \rho v_{pn}^2 &= \rho v_{p0}^2 \sqrt{(1 + 2\delta)} \\ (C_{33} + C_{44})^2 &= \rho^2 (v_{p0}^2 - v_{s0}^2)(v_{pn}^2 - v_{s0}^2)\end{aligned}\tag{15}$$

the first-order Pseudo-pure-mode qSV-wave equations can be rewritten as below:

$$\begin{aligned}\rho \frac{\partial \sigma_{xx}}{\partial t} &= (1 + 2\epsilon)\rho v_{p0}^2 \frac{\partial v_x}{\partial x} \\ \rho \frac{\partial \sigma_{zz}}{\partial t} &= \rho v_{p0}^2 \frac{\partial v_z}{\partial z} \\ \rho \frac{\partial \sigma_{xz}}{\partial t} &= \rho v_{s0}^2 \frac{\partial v_x}{\partial z} - \sqrt{\rho^2 (v_{p0}^2 - v_{s0}^2)(v_{pn}^2 - v_{s0}^2)} \frac{\partial v_z}{\partial z} \\ \rho \frac{\partial \sigma_{zx}}{\partial t} &= \rho v_{s0}^2 \frac{\partial v_z}{\partial x} - \sqrt{\rho^2 (v_{p0}^2 - v_{s0}^2)(v_{pn}^2 - v_{s0}^2)} \frac{\partial v_x}{\partial x} \\ \rho \frac{\partial v_x}{\partial t} &= \frac{\partial \sigma_{xx}}{\partial x} + \frac{\partial \sigma_{xz}}{\partial z} \\ \rho \frac{\partial v_z}{\partial t} &= \frac{\partial \sigma_{zx}}{\partial x} + \frac{\partial \sigma_{zz}}{\partial z}\end{aligned}\tag{16}$$

Following the principle of staggered-grid scheme in 2D qSV and SH wave propagators proposed by Virieux (1984, 1986), σ_{xx} and σ_{zz} , σ_{xz} and σ_{zx} are respectively distributed at

the same grid points, which are indicated in Figure 1. Having applied above procedures, we are now ready to use variables v_x , v_z , σ_{xx} , σ_{zz} , σ_{xz} and σ_{zx} as conjugate physical quantities distributed on staggered grid. After the adoption of staggered-grid scheme to equation 13 and equation 14, the explicit differential iteration algorithm is obtained, which is very similar to those of elastic wave equations.

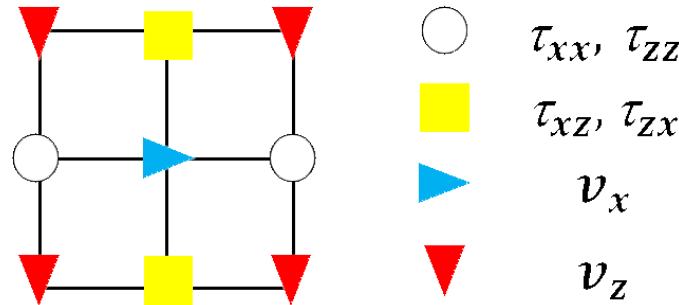


FIG. 1. 2D Staggered Grid

What's also worthy to note is that v_x and v_z are not distributed at the same grid point, therefore v_z field of every grid needs to be taken further care of to correspond to v_x field. To be specific, when the force source is loaded at v_x , corresponding v_z field should be averaged by 4 v_z fields surrounding the v_x field (Liu et al., 2017). Besides, the first-order Hybrid-PML proposed by Zhang et al. (2014) can be directly implemented in this first-order finite difference algorithm. The stretching factor is expressed as:

$$s_x = \frac{d_x + m_{x/z}d_z}{\alpha_x + i\omega} \quad (17)$$

Correction of Projection Deviation of qSV-Mode Waves

In VTI media, the polarizations of P- and SV-mode waves are no longer parallel or perpendicular to the propagation direction (Dellinger and Etgen, 1990, Dellinger, 1991), so they are called 'quasi-P' and 'quasi-SV' waves. Since qP- and qSV-mode waves in VTI media are intrinsically coupled, there will still be some residual qP-wave energy in the wavefields simulated by the first-order pseudo-pure-mode qSV-wave equations. Therefore, the correction of polarization directions of simulated wavefields needs to be performed, the strategy is to further project simulated wavefields onto the anisotropic references of polarization direction by applying spatial domain deviated operators designed by Cheng and Kang (2016), which will completely remove residual qP-mode wave energy.

Simulation Examples of Separated Scalar qSV-Waves

Homogeneous isotropic medium

In this paper, series of simulation examples will be presented. For comparison, we performed the numerical simulation of qSV-mode wave propagation with both original elastic wave equations and first-order pseudo-pure-qSV-mode wave equations proposed in

this study. The accuracy of the finite-difference schemes is set to $O(\Delta t^2 + \Delta x^4)$ (Levander, 1988). In the first case, we apply the algorithms to a homogeneous isotropic medium with size of $2km \times 2km$, whose density is 2500 kg/m^3 , P-wave velocity is 4000 m/s and S-wave velocity is 2300 m/s , force source is loaded at v_x grid point right in the middle of the model. The normalized x - and z -components of wavenumber K for a homogeneous isotropic medium is shown in Figure 2, which are also the polarization direction components of P-mode wave.

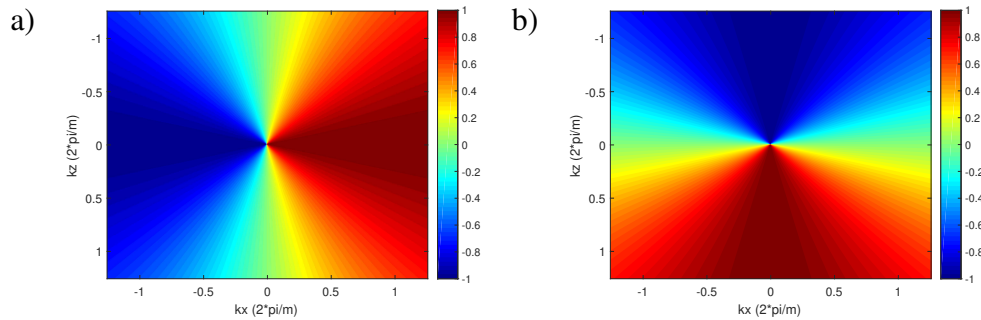


FIG. 2. Normalized wavenumber-domain operators in 2D isotropic medium: a) k_x and b) k_z .

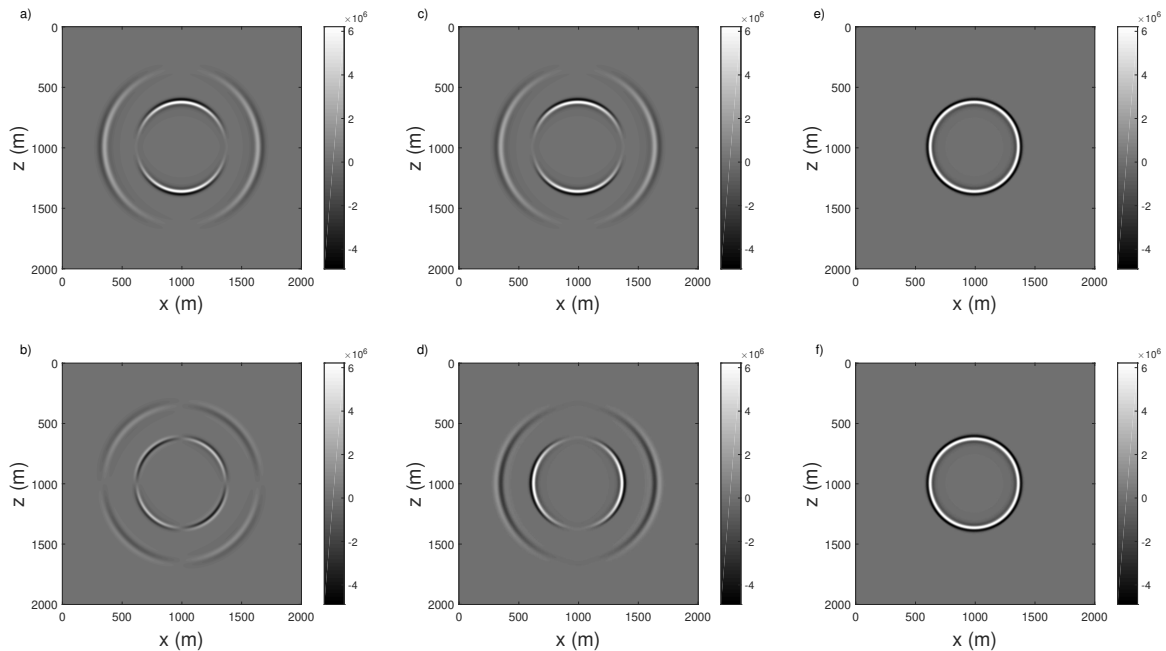


FIG. 3. Synthetic wavefields in an isotropic medium: a) x - and b) z -component simulated by original elastic wave equations; c) x - and d) z -components simulated by first-order pseudo-pure-mode qSV-wave equations; e) pseudo-pure-mode scalar qSV-wave field; f) separated scalar qSV-wave field.

The snapshots of synthetic qSV-wavefields are shown in Figure 3. a) and b) are x - and z -components simulated by original elastic wave equations, respectively. c) and d) are x - and z -components simulated by first-order pseudo-pure-mode qSV-wave equations, respectively. We can see the x - and z -components of qP-wave are in totally opposite phase, which enhances qSV-waves by summing up the components; e) is the summation of x -

and z -components which eliminates residual qP-wave energy and leads to a scalar pseudo-pure-mode qSV-wave field; f) is scalar qSV -wavefield filtered with deviation operators, which is the identical with e). because qSV-mode wave propagate perpendicularly to the polarization direction and $a^P = K$ in an isotropic medium case.

Homogeneous VTI medium with weak anisotropy

In this case, we apply the algorithms to a homogeneous VTI medium with weak anisotropy, whose $vp_0 = 3000m/s$, $vs_0 = 1500m/s$, $\epsilon = 0.1$ and $\delta = 0.05$ (Cheng and Kang, 2013, 2016). The normalized x - and z -component of polarization vector of qP-waves in the homogeneous VTI medium is shown in Figure 4. The normalized x - and z -components of wavenumber domain and spatial domain deviation operators are shown in Figure 5 and Figure 6, respectively.

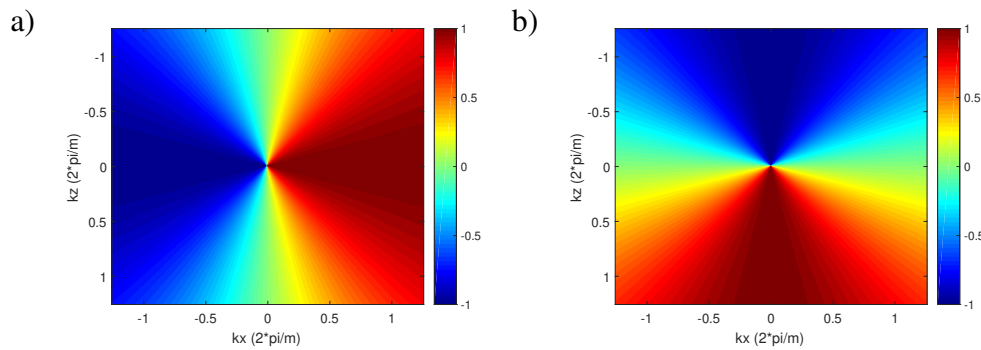


FIG. 4. Normalized wavenumber-domain operator in 2D VTI medium with weak anisotropy: a) x - and b) z -component of polarization vector of qP-mode wave.

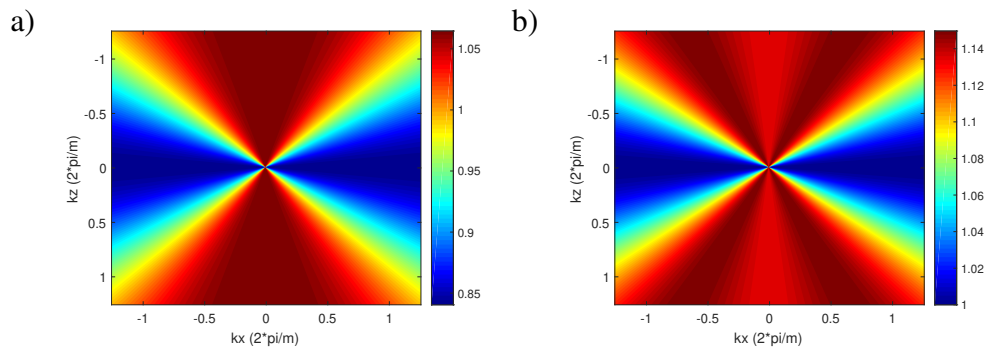


FIG. 5. Normalized wavenumber-domain operator in 2D VTI medium with weak anisotropy: a) x - and b) z -component of deviation operator.

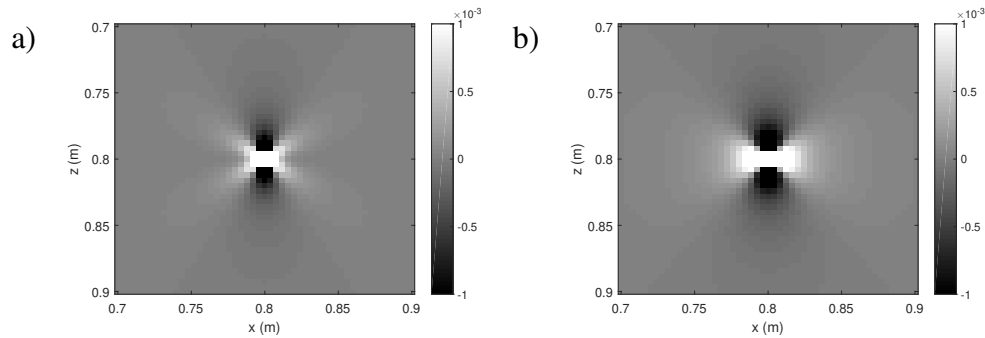


FIG. 6. Spatial domain deviation operator in 2D VTI medium with weak anisotropy: a) x-component; b) z-component.

The snapshots of synthetic qSV-wavefields in VTI medium are shown in Figure 7: a) and b), c) and d) are respectively the x - and z -components of the velocity wavefields simulated by original elastic wave equations and first-order pseudo-qSV-mode equations. The x - and z -components of qP-wavefields in c) and d) are in different phases, the summation e) enhances qSV-mode waves in VTI media, while leaving some residual qP-mode energy in the physical domain. Then we perform the filtering algorithm to the synthetic wavefields, as shown in f) is the separated scalar qSV-wavefield, where qP-mode energy is completely removed with the projection deviation correction.

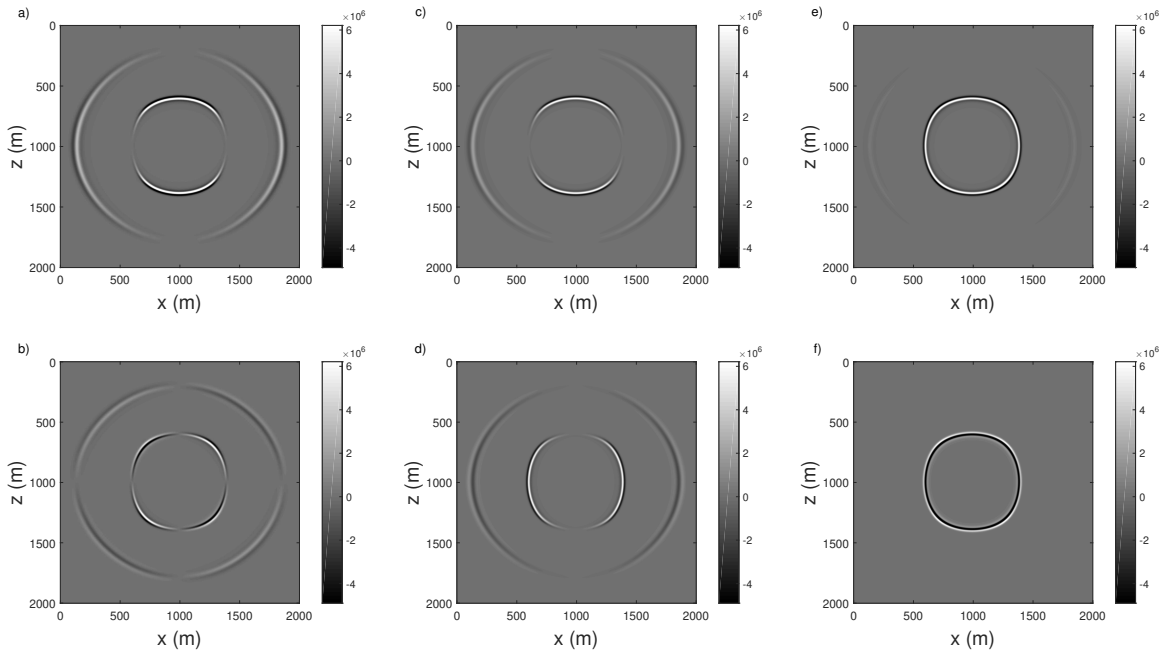


FIG. 7. Synthetic wavefields in a VTI medium with weak anisotropy: a) x- and b) z-component simulated by original elastic wave equations; c) x- and d) z-component simulated by first-order pseudo-pure-mode qSV-wave equations; e) pseudo-pure-mode scalar qSV-wave field; f) separated scalar qSV-wave field.

Homogeneous VTI medium with strong anisotropy

In the third case, we apply the new algorithm to a VTI medium with strong anisotropy, whose elastic parameters: C_{11} is 23.87 GPa, C_{33} is 15.33 GPa, C_{13} is 9.79 GPa, C_{44} is 2.77 GPa and density is $2500\text{kg}/\text{m}^3$. The snapshots of synthetic qSV-wavefields are shown in Figure 8. From the comparison between Figure 8 e) and f), we can see the qP-mode energy can also be completely eliminated and scalar pseudo-qSV-mode wave can be obtained from this algorithm.

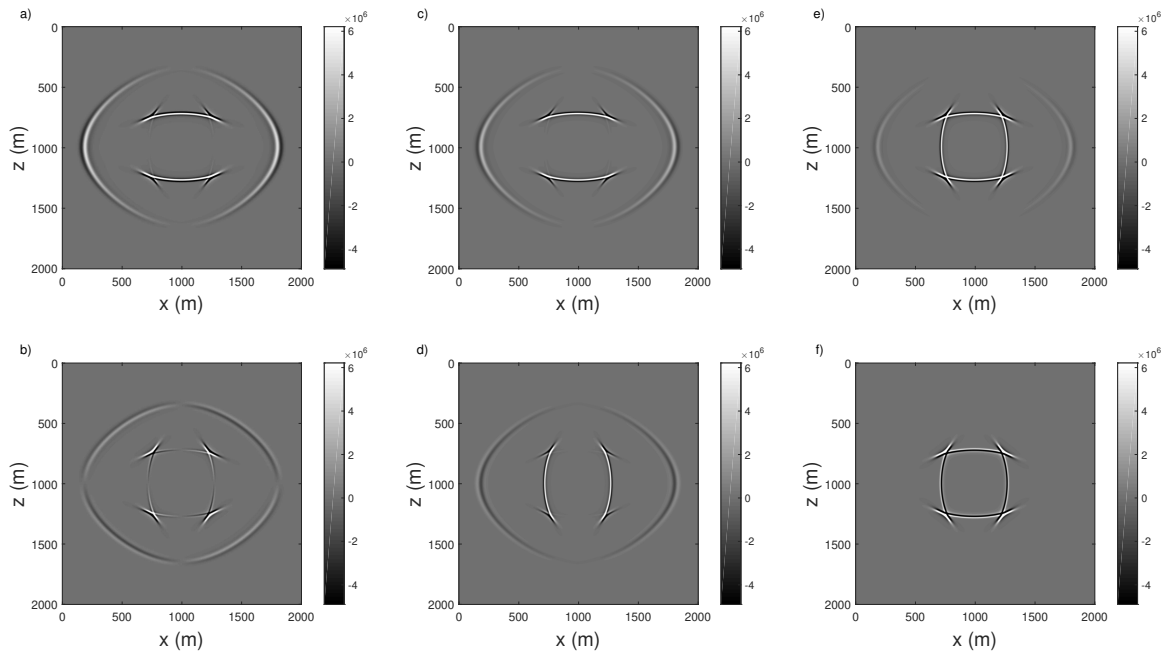


FIG. 8. Synthetic wavefields in a VTI medium with strong anisotropy: a) x- and b) z-component simulated by original elastic wave equations; c) x- and d) z-component simulated by first-order pseudo-pure-mode qSV-wave equations; e) pseudo-pure-mode scalar qSV-wave field; f) separated scalar qSV-wave field.

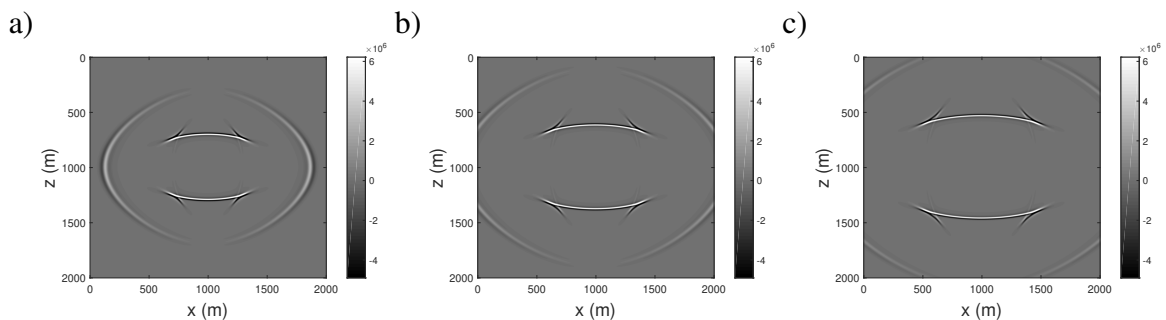


FIG. 9. Snapshots of x-component simulated by first-order pseudo-pure-mode qSV-wave equations in a VTI medium with strong anisotropy: a) 320 ms, b) 400 ms and c) 480 ms, respectively.

To test the applicability of first-order Hybrid-PML (Zhang et al., 2014; Liu et al., 2017) in the new algorithm, the snapshots of synthetic qSV-wavefields simulated by first-order Pseudo-pure-mode qSV-wave equations propagating at different time are presented. As

shown in Figure 9 a), b) and c) are the snapshots of x -component of qSV-wavefields propagating at 320 ms, 400 ms and 480 ms, respectively. As observed from the snapshots, the energy at the boundary can be efficiently absorbed and no artificial reflections emerge, which demonstrates that Hybrid-PML can be implemented in our algorithm with excellent performance.

Heterogeneous layered VTI media

In this section, the new algorithm is applied to a heterogeneous two-layered VTI model, in which the first and the second layer are the same VTI medium with strong and weak anisotropy, respectively. A force source is set right in the middle of the model with the interface at the depth of 1.2 km. Snapshots of synthetic qSV-wavefields are shown in Figure 10. We can see both of qP-wave and qSV-wave lead to converted S-wavefields when they reach at the interface. By the summation of x - and z -components of synthetic qSV-wavefields shown in Figure 10 e), some of converted wavefields are already seriously suppressed. While after the correction of polarization direction, all residual qP-mode energy is eliminated and pure scalar qSV-mode wave is obtained as shown in Figure 10 f). From the comparison between Figure 10 e) and f), it's demonstrated that with further polarization-based correction not only is qP-mode energy eliminated, but also the converted P-wave energy.

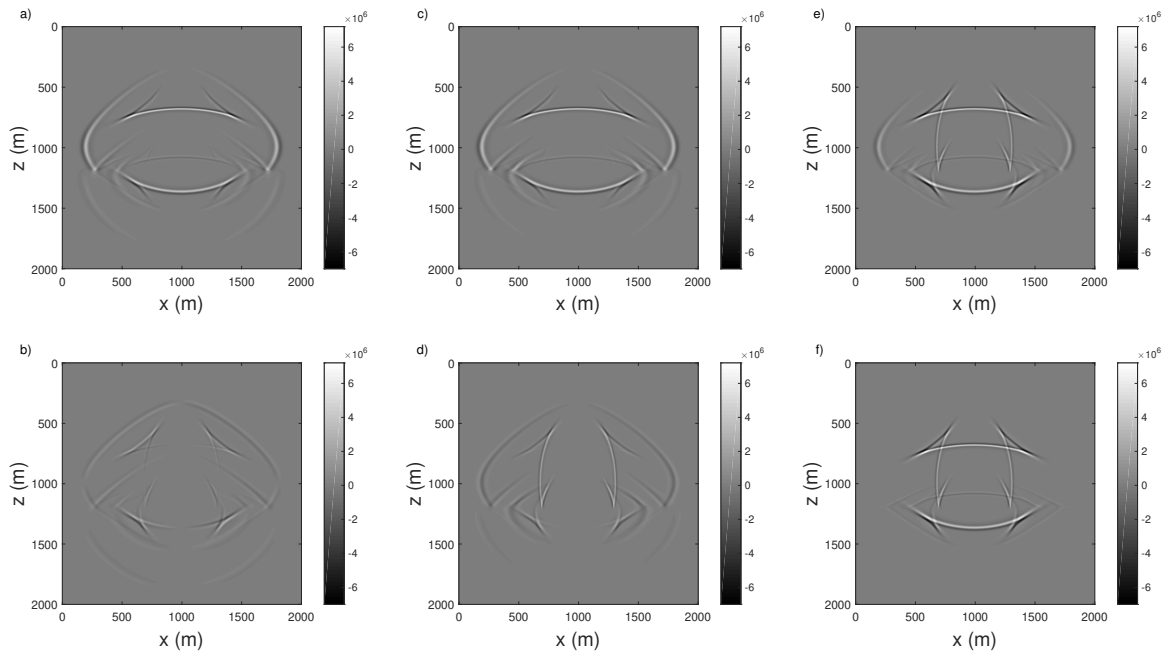


FIG. 10. Synthetic wavefields in a layered VTI model with strong anisotropy in the first layer and weak anisotropy in the second layer: a) x - and b) z -component simulated by original elastic wave equations; c) x - and d) z -component simulated by first-order pseudo-pure-mode qSV-wave equations; e) pseudo-pure-mode scalar qSV-wave field; f) separated scalar qSV-wave field.

Heterogeneous Hess VTI model

In the final example, we apply the new algorithm to part of the heterogeneous SEG/Hess VTI model, whose elastic parameters are shown in Figure 11. For a heterogeneous model, all spatial domain deviation operators for each medium need to be calculated with their elastic parameters or Thomsen parameters.

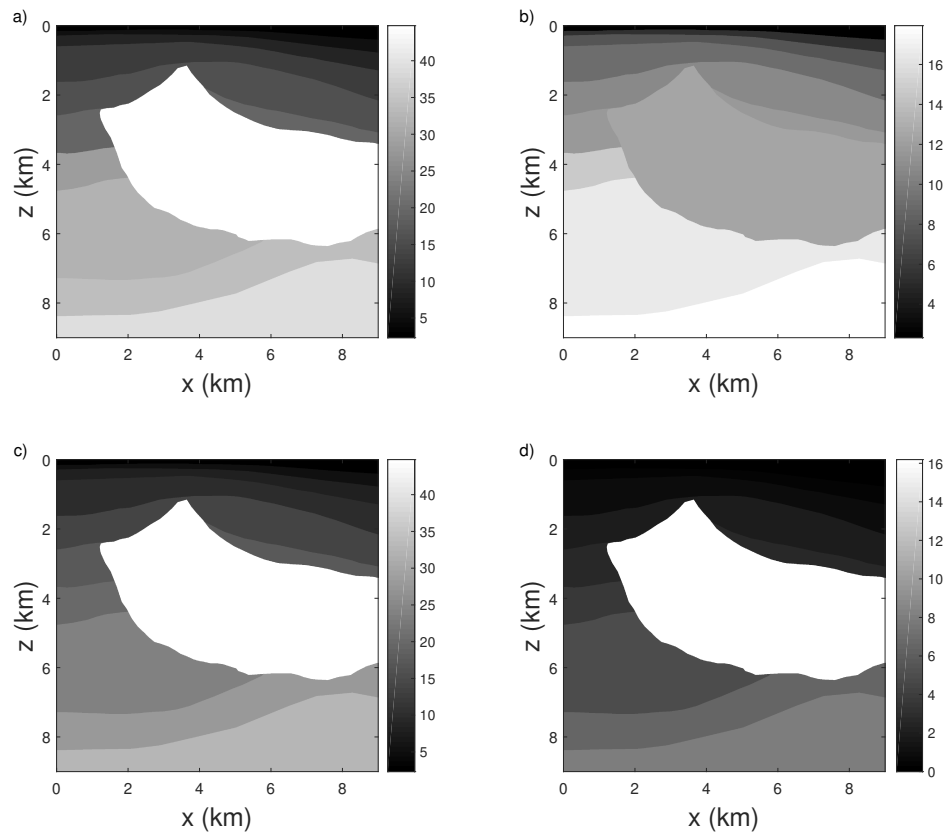


FIG. 11. Part of SEG/Hess VTI model: a) C_{11} , b) C_{13} , c) C_{33} and d) C_{44} .

As shown in Figure 12 are the synthetic qSV-wavefields, from which we can observe that after the summation of x - and z - components, qP-mode wave energy has already been extremely suppressed and the summed wavefields (i.e., pseudo-pure-mode scalar qSV-wavefields) contain quite weak residual qP-wave energy. As Cheng and Kang (2013) pointed out, compared to separated scalar qSV-mode waves shown in Figure 12 d), the summed wavefields without performing further spatial filtering to eliminate residual qP-wave energy may also result in potentially reasonable ERTM results.

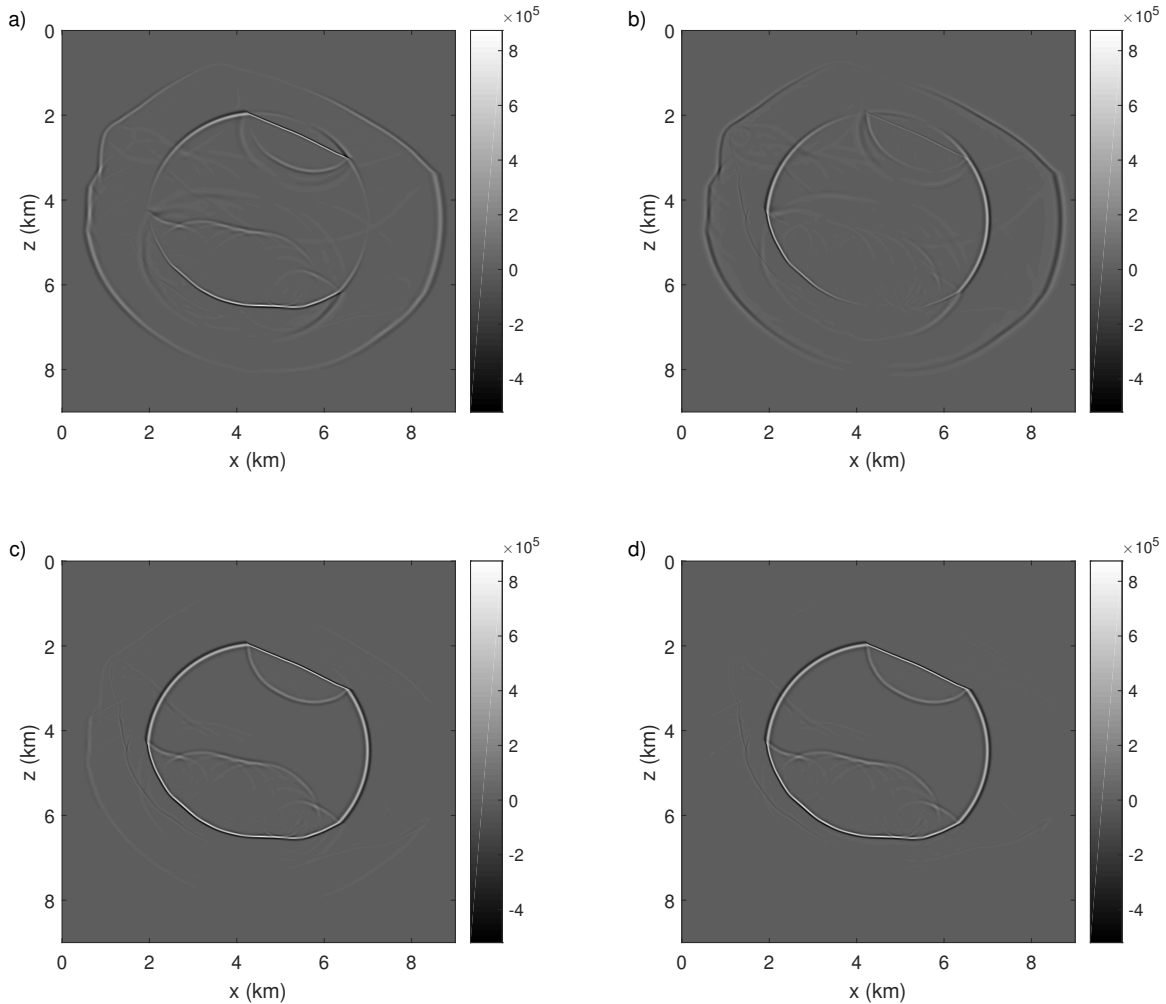


FIG. 12. Synthetic wavefields in SEG/Hess VTI model: a) x- and b) z-component simulated by first-order pseudo-pure-mode qSV-wave equations; c) pseudo-pure-mode scalar qSV-wave field; d) separated scalar qSV-wave field.

DISCUSSION

Yan and Sava (2008b) proposed to perform the RTM algorithms to separated scalar wavefields using cross-correlation imaging conditions. Our algorithm is an alternative approach for the simulation of pseudo-pure-qSV-mode waves in general 2D VTI media. The similarity transform introduced to Christoffel matrix can preserve the kinematics of qSV-wave propagation (Cheng and Kang, 2016). Unlike second-order equations simulated by extrapolation methods, first-order equations are employed with staggered grid scheme in our algorithm, velocity fields rather than displacement fields are obtained from the simulation procedure. Fortunately, qSV-mode waves not only can be separated from displacement fields, but also from velocity and stress fields, which is very similar to wave vector decomposition method (Zhang and McMechan, 2010). Since the first-order pseudo-pure-mode qSV-wave equations are very similar to those of first-order elastic wave equations, we can achieve the new algorithm with simple modification to existing first-order elastic wave simulation algorithms. In 2D staggered grid, v_x and v_z grid points are half a grid away from

each other in both x - and z -axis directions. Therefore, v_z field should be phase shifted before the filtering algorithm is performed. Alternatively, when the force source is loaded at v_x , we can simply average 4 corresponding v_z fields surrounding the v_x field (Liu et al., 2017), which can also provide sufficient accuracy. Consistent with wavefield separation procedures (Dellinger and Etgen, 1990; Dellinger, 1991; Yan and Sava, 2008a, 2009), our algorithm will also change the phase and amplitude of qSV-waves inevitably. As for absorbing boundary condition, the first-order Hybrid-PML proposed by Zhang et al. (2014) and Liu et al. (2017) can be directly implemented in this first-order finite difference algorithm, which achieves better efficiency with thinner PML layers and reduces the computational cost. Conventional finite difference method approximated with Taylor series expansion still suffers from dispersion problem with big large size and time step, therefore, this algorithm may show better performance with other more efficient approximation methods. For instance, since first-order pseudo-pure-qSV-mode wave equations have been derived, we may perform simulation procedure with pseudospectral method (Li et al., 2018).

CONCLUSIONS

In this study, we have proposed a first-order pseudo-pure-qSV-mode wave propagator in 2D VTI media. This qSV-wave propagator can be employed in numerical simulation with finite difference method using variables v and σ as conjugate physical quantities distributed on staggered grid. We have performed the proposed algorithm to homogeneous isotropic medium, which can provide scalar qSV-mode waves by simply summarizing x - and z -components. Also, we have presented synthetic examples of homogeneous anisotropic VTI medium with weak/strong anisotropy, heterogeneous layered VTI model and part of SEG/Hess VTI model, the synthetic wavefields of which need to be further projected onto local anisotropic references to remove residual qP-wave energy. Through the simulation examples, it's demonstrated that the algorithm is capable of simulating pseudo-pure-qSV-mode wave propagation with further polarization-based projection. In addition, the snapshots of x -component at different time demonstrated that Hybrid-PML can be efficiently implemented in this algorithm.

ACKNOWLEDGMENTS

We thank the sponsors of CREWES for continued support. This work was funded by CREWES industrial sponsors, and NSERC (Natural Science and Engineering Research Council of Canada) through the grant CRDPJ 461179-13.

REFERENCES

- Aki, K., and Richards, P. G., 2002, Quantitative seismology:
- Cheng, J., and Kang, W., 2013, Simulating propagation of separated wave modes in general anisotropic media, part i: qp-wave propagators: *Geophysics*, **79**, No. 1, C1–C18.
- Cheng, J., and Kang, W., 2016, Simulating propagation of separated wave modes in general anisotropic media, part ii: qs-wave propagators: *Geophysics*, **81**, No. 2, C39–C52.
- Dellinger, J., and Etgen, J., 1990, Wave-field separation in two-dimensional anisotropic media: *Geophysics*, **55**, No. 7, 914–919.
- Dellinger, J. A., 1991, Anisotropic seismic wave propagation, vol. 69: Stanford University Stanford.

- Dickens, T. A., and Winbow, G. A., 2011, Rtm angle gathers using poynting vectors, *in* SEG Technical Program Expanded Abstracts 2011, Society of Exploration Geophysicists, 3109–3113.
- Jianlei, Z., Zhenping, T., and Chengxiang, W., 2007, P-and s-wave-separated elastic wave-equation numerical modeling using 2d staggered grid, *in* SEG Technical Program Expanded Abstracts 2007, Society of Exploration Geophysicists, 2104–2109.
- Levander, A. R., 1988, Fourth-order finite-difference p-sv seismograms: *Geophysics*, **53**, No. 11, 1425–1436.
- Li, J., Innanen, K. A., and Tao, G., 2018, A 3d pseudo-spectral method for sh wave simulation in heterogeneous media, *in* SEG Technical Program Expanded Abstracts 2018, Society of Exploration Geophysicists, 4005–4009.
- Liu, H., Wang, B., Ali, M., Tao, G., Yue, W., and Sun, H., 2018, A first-order qsv-wave propagator in 2d vti media, *in* 80th EAGE Conference and Exhibition 2018.
- Liu, H., Wang, B., Tao, G., Zhang, K., and Yue, W., 2017, Study on the simulation of acoustic logging measurements in horizontal and deviated wells: *Applied geophysics*.
- Morse, P. M., and Feshbach, H., 1954, Methods of theoretical physics: *American Journal of Physics*, **22**, No. 6, 410–413.
- Rommel, B. E., 1994, Approximate polarization of plane waves in a medium having weak transverse isotropy: *Geophysics*, **59**, No. 10, 1605–1612.
- Thomsen, L., 1986, Weak elastic anisotropy: *Geophysics*, **51**, No. 10, 1954–1966.
- Tsvankin, I., 2012, Seismic signatures and analysis of reflection data in anisotropic media: Society of Exploration Geophysicists.
- Virieux, J., 1984, Sh-wave propagation in heterogeneous media: Velocity-stress finite-difference method: *Geophysics*, **49**, No. 11, 1933–1942.
- Virieux, J., 1986, P-sv wave propagation in heterogeneous media: Velocity-stress finite-difference method: *Geophysics*, **51**, No. 4, 889–901.
- Yan, J., and Sava, P., 2008a, Elastic wavefield separation for vti media, *in* SEG Technical Program Expanded Abstracts 2008, Society of Exploration Geophysicists, 2191–2195.
- Yan, J., and Sava, P., 2008b, Isotropic angle-domain elastic reverse-time migration: *Geophysics*, **73**, No. 6, S229–S239.
- Yan, J., and Sava, P., 2009, Elastic wave-mode separation for vti media: *Geophysics*, **74**, No. 5, WB19–WB32.
- Yoon, K., and Marfurt, K. J., 2006, Reverse-time migration using the poynting vector: *Exploration Geophysics*, **37**, No. 1, 102–107.
- Zhang, K., Tao, G., Li, J., Wang, H., Liu, H., and Ye, Q., 2014, 3d fdm modeling of acoustic reflection logging in a deviated well, *in* 76th EAGE Conference and Exhibition 2014.
- Zhang, Q., and McMechan, G. A., 2010, 2d and 3d elastic wavefield vector decomposition in the wavenumber domain for vti media: *Geophysics*, **75**, No. 3, D13–D26.
- Zhou, Y., and Wang, H., 2016a, Efficient wave mode separation in anisotropic media-part i-separation operators, *in* 78th EAGE Conference and Exhibition 2016.
- Zhou, Y., and Wang, H., 2016b, Efficient wave-mode separation in vertical transversely isotropic media: *Geophysics*, **82**, No. 2, C35–C47.